Journal of Solid State Chemistry 184 (2011) 2640–2647

Contents lists available at ScienceDirect

Journal of Solid State Chemistry

journal homepage: www.elsevier.com/locate/jssc

New phases in the system $LiMnVO_4$–$Mn_3(VO_4)_2$

Oliver Clemens [a], Robert Haberkorn [b], Horst Philipp Beck [a,*]

[a] Universität des Saarlandes, Institut für Anorganische und Analytische Chemie und Radiochemie, Am Markt, Zeile 5, 66125 Saarbrücken, Germany
[b] Universität des Saarlandes, Anorganische Festkörperchemie, Am Markt, Zeile 3, 66125 Saarbrücken, Germany

ARTICLE INFO

Article history:
Received 24 May 2011
Received in revised form
24 July 2011
Accepted 26 July 2011
Available online 3 August 2011

Keywords:
Lithium manganese vanadate
Manganese vanadate
Rietveld
$Mn_3V_2O_8$
$Mn_3(VO_4)_2$
Phase transition

ABSTRACT

The synthesis of orthorhombic $Mn_3(VO_4)_2$ via a simple solid state route as well as the description of a new tetragonal high temperature phase are reported in this paper. Additionally, the system $LiMnVO_4$–$Mn_3(VO_4)_2$ (=$Mn_{1.5}VO_4$), described by the formula $Li_xMn_{1.5-x/2}VO_4$, is investigated in detail, showing that substitution of one Mn^{2+} in $Mn_{1.5}VO_4$ by two Li^+ ions favors the formation of the tetragonal high temperature phase for $x \leq 0.22$. This substitution is facilitated by the statistical half occupancy of the 4*b* site by Mn^{2+} in tetragonal $Mn_{1.5}VO_4$, whereas additional crystallographic sites would have to be occupied in the orthorhombic phase. The inverse substitution of Li by Mn in orthorhombic $LiMnVO_4$ is also shown to be possible in the range $0.72 \leq x \leq 1$. For $0.22 \leq x \leq 0.72$, there is a large miscibility gap with a two phase mixture of the tetragonal $Mn_{1.5}VO_4$ type and orthorhombic $LiMnVO_4$ type phases.

1. Introduction

Olivine type phases with the general formula $LiMPO_4$ (*M*=Fe, Mn, Co, Ni) [1–7] are promising cathode materials for the use in lithium ion batteries, especially for *M*=Fe and Mn [2]. $LiMnVO_4$ is reported to crystallize in the orthorhombic Na_2CrO_4 type structure with space group *Cmcm* [8–15], being isotypic with $LiMgVO_4$ [10,16–18] and $Li_{1.2}In_{0.6}VO_4$ [19]. The structure (Fig. 1) is made up of isolated VO_4 tetrahedra forming a distorted cubic close packed arrangement of oxygen atoms. In contrast to the spinel type materials $Li^{[6]}Co^{[6]}V^{[4]}O_4$ [11,20,21] and $Li^{[6]}Ni^{[6]}V^{[4]}O_4$ [11,22,23] (coordination numbers for the ions shown in superscript parentheses), Li is located on a tetrahedral site. These tetrahedra share an edge with the VO_4 ones. Mn is located in an octahedral site, sharing vertices with the VO_4 tetrahedra and building up chains of octahedra sharing edges among each other. Thus, the orthorhombic phase may be written as $Li^{[4]}Mn^{[6]}V^{[4]}O_4$. Although Li cannot be extracted from this phase, the high pressure spinel-type modification hp-$Li^{[6]}Mn^{[6]}V^{[4]}O_4$ allows the reversible extraction of about 0.6 Li at a voltage of 3.8 V [8], which is slightly lower compared to a voltage of about 4.0 V in $LiMnPO_4$ [2]. Although the electrical conductivity of orthorhombic $LiMnVO_4$ is lower compared to that of the spinel-type compounds $LiCoVO_4$ and $LiNiVO_4$ [11], it is still higher by about 5–6 orders of magnitudes compared to $LiMnPO_4$ [24].

There are only few reports about $Mn_3(VO_4)_2$ (from now on written as $Mn_{1.5}VO_4$ to clarify the similarity to $LiMnVO_4$). Clark et al. [25] reported that they could not synthesize pure $Mn_{1.5}VO_4$. They explain this observation with instability of that phase decomposing easily to $Mn_2V_2O_7$ and $Mn_4V_2O_9$. X-ray powder diagrams of the latter could not be indexed and a structural characterization was not possible. However, such a phase was also reported by Brisi [26]. Single crystals of $Mn_{1.5}V_{0.94}Mo_{0.04}O_4$ were grown by Wang et al. [27] from a eutectic mixture of $Mn_{1.5}VO_4$ and $MnMoO_4$. They reported this phase to crystallize in an orthorhombic structure (Fig. 2) with space group *Cmca* (not to be mixed up with the structure of $LiMnVO_4$ in space group *Cmcm*, which is clearly different). Mn occupies two crystallographically different octahedral sites (4*a*, 8*e*); V is on the tetrahedral site 8*e* in a distorted ccp arrangement of the oxygen atoms. $Mn_{1.5}VO_4$ is therefore isotypic with other divalent (transition) metal vanadates $M_{1.5}VO_4$ (*M*=Mg, Co, Ni, Zn) [16,28–33].

In this paper, we report on the first synthesis of pure phase orthorhombic $Mn_{1.5}VO_4$ (with space group *Cmca*) via a simple solid state route as well as a new tetragonal high temperature phase of $Mn_{1.5}VO_4$ and solid solutions of the latter with $LiMnVO_4$.

2. Experimental

For the synthesis of the low temperature phase of $Mn_3(VO_4)_2$ (=$Mn_{1.5}VO_4$), stoichiometric amounts of MnO (99%, Alfa Aesar) and V_2O_5 (99.6+%, Aldrich) were milled for 2 h in a planetary ball mill (Fritsch pulverisette 7) at a speed of ~440 rpm. The as-received

* Corresponding author. Fax: +49 681 3024233.
E-mail address: hp.beck@mx.uni-saarland.de (H.P. Beck).

0022-4596/$ - see front matter © 2011 Elsevier Inc. All rights reserved.
doi:10.1016/j.jssc.2011.07.042

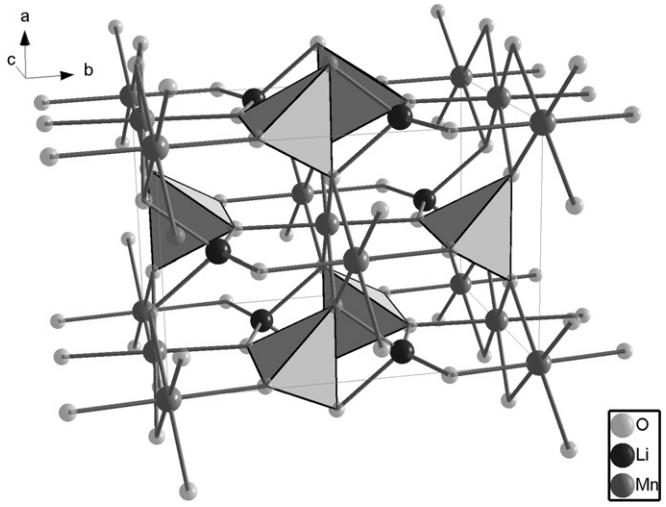

Fig. 1. The crystal structure of $LiMnVO_4$ according to Padhi [8]. Vanadium is located in the solid tetrahedra.

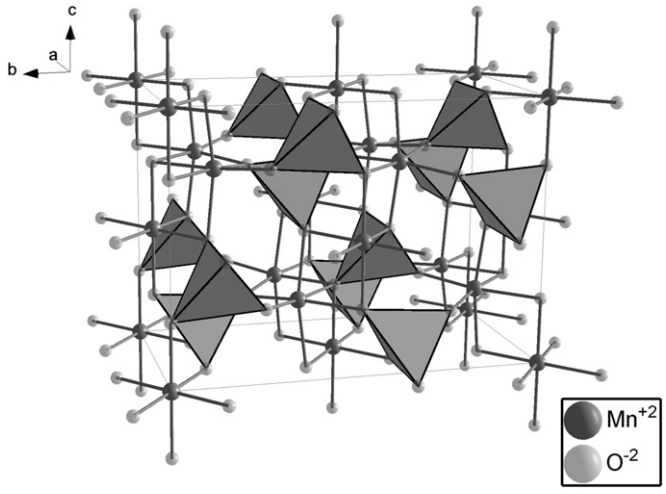

Fig. 2. The crystal structure of $Mn_{1.5}VO_4$ according to Wang [27]. V^{5+} is located in the solid tetrahedra.

powder (LT phase) was pressed into a pellet and heated to 800 °C for 15 h under dry flowing Ar of purity 4.6. The high temperature phase of $Mn_{1.5}VO_4$ was made by heating the low temperature phase to a temperature of 950 °C for 15 h in an alumina or Pt boat, again under flowing Ar (purity 4.6). A second boat, filled with MnO and placed in front of the boat with the reaction pellet/mixture in the direction of the Ar flux, allowed a further purifying of the Ar atmosphere from traces of O_2/H_2O.

Samples of composition $Li_xMn_{1.5-x/2}VO_4$ were made from stoichiometric amounts of Li_2CO_3 (99+%, Aldrich), MnO (99%, Alfa Aesar) and V_2O_5 (99.6+%, Aldrich), also by use of the planetary ball mill. The samples were heated in Pt boats under dry flowing Ar (purity 4.6), depending on the value of x, to temperatures varying between 850 and 950 °C, with 1 intermediate regrinding. Lower temperatures were preferably chosen for Li richer samples to avoid melting. Again, a second boat filled with MnO was placed in front of the one containing the reaction mixture. According to our experience, the chosen temperature treatments do not cause any loss of lithium and even further treatment at the maximal chosen temperature does not result in any changes of the refined sample composition and determined lattice parameters.

XRD patterns were recorded on a Panalytical Philips X'Pert Pro diffractometer with focusing Bragg–Brentano geometry and a fine focus X-ray tube with Cu anode in a 2θ-range from 10° to 140°. No primary beam monochromator was attached. A fast PIXcel detector and a variable divergence slit were used. The total scan time was between 3 and 14 h.

The whole 2θ-range was used for Rietveld analysis by the program TOPAS 2.1 [34] (Bruker AXS, Karlsruhe, Germany). The instrumental intensity distribution and peak shape parameters were determined empirically according to the fundamental parameters set [35] after a reference scan of LaB_6. Positional parameters, microstructural and lattice parameters were refined during Rietveld analysis. To refine microstructural parameters, the program TOPAS [34] uses a double Voigt model. For multiphase mixtures, the displacement parameters of all atoms of all phases were constraint to an overall B-value to minimize errors of phase quantification. For single phase samples, the structural model of the according phase was constrained to a composition $Li_xMn_{1.5-x/2}VO_4$, and x was refined accordingly. Indexing [36] and Fourier difference analysis of the pattern of the high temperature phase of $Mn_{1.5}VO_4$ were done using the program TOPAS 4.2 [37] (Bruker AXS, Karlsruhe, Germany). Based on our experience, the standard deviations for the lattice parameters given in this article are the ones calculated by the Rietveld procedure multiplied by 4.

The DTA measurement was recorded on a Netzsch DTA/TG (STA 409) up to a temperature of 1020 °C with a heating and cooling rate of 5 °C/min under a flowing Ar atmosphere.

3. Results and discussion

3.1. On $Mn_3(VO_4)_2$ ($=Mn_{1.5}VO_4$)

Sample preparation has a high influence on the phase purity of the received $Mn_{1.5}VO_4$. Using a ball mill and compacting the powder into a tablet gave a product with a significantly lower amount of impurity phase. Also, placing a boat with fine ground powder of MnO into the furnace helped to avoid the oxidation of the Mn^{2+} in the product by traces of O_2. The reaction temperature was chosen to be 800 °C. Following this procedure yielded a product with a negligible amount of $Mn_2V_2O_7$ (about 1.2%). The diffraction pattern of the as received powder is given in Fig. 3a, the structural results of the refinement, which are in good agreement with the results of Wang et al. for their Mo doped $Mn_{1.5}VO_4$ phase, are given in Table 1. The refined M–O distances (Table 2) are in excellent agreement with the sum of the ionic radii of the different ionic species [38].

Since Clark [25] reports the decomposition of orthorhombic $Mn_{1.5}VO_4$ when raising the reaction temperature, the sample was heated to 950 °C in an alumina boat. Indeed, also in this work, a complete disappearance of the orthorhombic $Mn_{1.5}VO_4$ was observed. A single new phase, with a diagram closely resembling the $Mn_4V_2O_9$ phase reported by Brisi [26] and Clark [25], appeared instead, but no impurities of $Mn_2V_2O_7$ could be detected. The result of the indexing indicates a tetragonal unit cell in the space group $I\bar{4}2d$ and lattice parameters $a=7.0073(1)$ Å and $c=19.6981(3)$ Å. A database [39] search for similar phases showed that $Co_{1.5}AsO_4$ [40], $Mg_{1.5}AsO_4$ [41], $Na_{1/3}Mg_{4/3}VO_4$ ($NaMg_4(VO_4)_3$) [42], $Li_{1/3}Mg_{4/3}VO_4$ ($LiMg_4(VO_4)_3$) [43–45] also crystallize in that space group with lattice parameters similar to the ones found for our new phase. Using the positional parameters of $Mg_{1.5}AsO_4$ [41] as starting parameters for the Rietveld refinement (Fig. 3b), the results (Table 3) confirm that this phase has the composition $Mn_{1.5}VO_4$ – and not $Mn_4V_2O_9$ – and that it is isostructural to $Co_{1.5}AsO_4$ [40] and $Mg_{1.5}AsO_4$ [41]. This is especially given by the refined approximate occupancy of the 4*b*

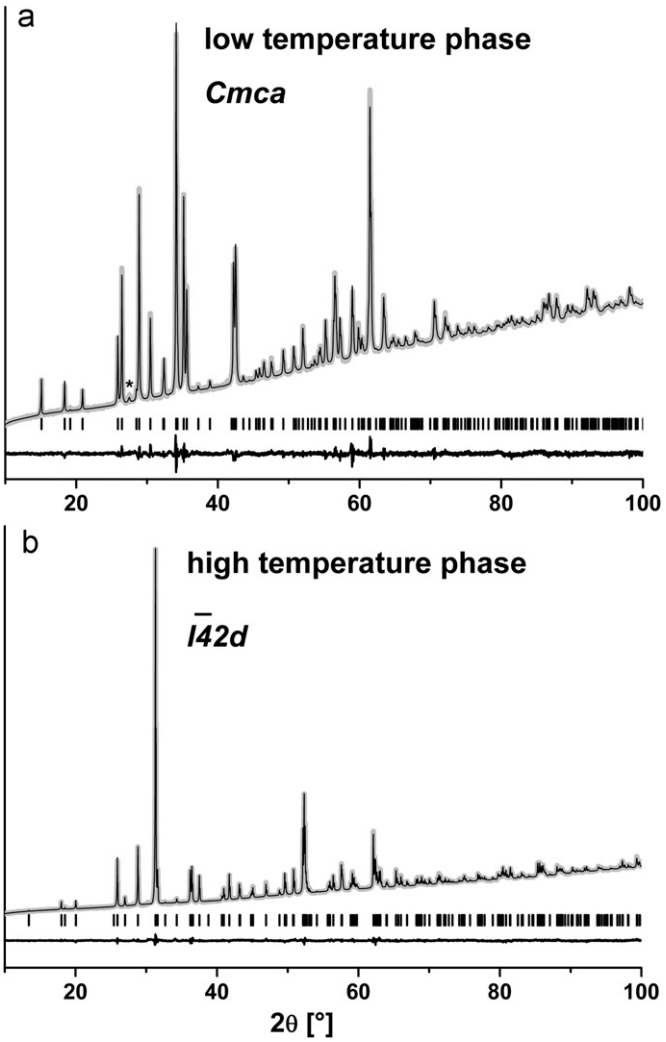

Fig. 3. Rietveld analysis of the XRD patterns of the synthesis product for the low (a) and high (b) temperature phases of $Mn_{1.5}VO_4$. Refined curve (black), measured curve (gray) and difference curve (black). The most intense reflection of the small amount of the impurity phase $Mn_2V_2O_7$ in (a) is marked with an asterisk. The background slope results from the varying divergence slit of the diffractometer.

Table 1
Results of the refinement for the low temperature phase of $Mn_{1.5}VO_4$, space group *Cmca*.

Wyckoff	Atom sort	*x*	*y*	*z*	Occupancy	*B*
4a	***Mn²⁺***	***0***	***0***	***0***	***1***	0.84(3)
8e	***Mn²⁺***	*1/4*	0.1376(1)	*1/4*	***1***	0.84(3)
8f	***V⁵⁺***	***0***	0.3795(1)	0.1217(2)	***1***	0.13(2)
8f	***O²⁻***	***0***	0.2565(3)	0.2234(3)	***1***	0.73(4)
8f	***O²⁻***	***0***	0.9997(3)	0.2496(4)	***1***	0.73(4)
16g	***O²⁻***	0.2802(3)	0.1174(2)	0.9927(2)	***1***	0.73(4)

a*[Å]**=6.2595(2), ***b*[Å]**=11.7254(4), ***c*[Å]**=8.4938(2), R_{wp}=0.99%, R_{Bragg}=0.55%, ***GOF=1.84.

Mn^{2+} site of about 0.5. This statistical disorder is also observed for $Co_{1.5}AsO_4$ [40] and $Mg_{1.5}AsO_4$ [41]. A Fourier difference analysis indicates that there is virtually no remarkable missing/excess electron density. This is also confirmed considering our synthesis attempts of phase pure $Mn_4V_2O_9$. In doing so, an additional unknown phase besides ht-$Mn_{1.5}VO_4$ was observed, which might be a yet unknown manganese richer phase in the system MnO–V_2O_5. Further investigations are clearly necessary to determine the detailed nature of that phase.

Table 2
Comparison of the refined *M*–O distances of the low temperature phase of $Mn_{1.5}VO_4$ (space group *Cmca*) to the sum of the ionic radii after Shannon [38] with *N* being the number of neighbors.

Atom site/atom sort	N	Refined distance (Å)	Average *M*–O distance (Å)	Sum of ionic radii [38]
4a*/*Mn²⁺	2	2.120(3)	2.193	2.187
	4	2.230(2)		
8e*/*Mn²⁺	2	2.108(3)	2.188	2.190
	2	2.206(2)		
	2	2.250(3)		
8f*/*V⁵⁺	1	1.681(4)	1.717	1.715
	2	1.685(2)		
	1	1.784(4)		

Table 3
Results of the refinement for the low temperature phase of $Mn_{1.5}VO_4$, space group $I\bar{4}2d$.

Wyckoff	Atom sort	*x*	*y*	*z*	Occupancy	*B*
8c	***Mn²⁺***	***0***	***0***	0.2269(1)	***1***	0.97(2)
8d	***Mn²⁺***	0.2403(2)	*1/4*	*1/8*	***1***	0.97(2)
4b	***Mn²⁺***	***0***	***0***	*1/2*	***0.491(3)***	0.97(2)
4a	***V⁵⁺***	***0***	***0***	***0***	***1***	0.42(2)
8d	***V⁵⁺***	0.6540(2)	*1/4*	*1/8*	***1***	0.42(2)
16e	***O²⁻***	0.0515(5)	0.1976(4)	0.0438(1)	***1***	1.57(4)
16e	***O²⁻***	0.0523(4)	0.2720(5)	0.3968(1)	***1***	1.57(4)
16e	***O²⁻***	0.4979(5)	0.2166(5)	0.0585(2)	***1***	1.57(4)

a*[Å]**=7.0073(1), ***c*[Å]**=19.6981(3), R_{wp}=0.86%, R_{Bragg}=0.42%, ***GOF=1.73.

In contrast to the orthorhombic modification of $Mn_{1.5}VO_4$, which has a distorted cubic close packing of the oxygen atoms, the tetragonal high temperature modification is built up by a distorted hexagonal close packing of oxygen atoms, where the layers are stacked along the [1 1 0] direction. The crystallographic density of 4.06 g/cm^3 is remarkably lower than that of the orthorhombic form (4.21 g/cm^3) as often found for high temperature phases. Table 4 summarizes the refined *M*–O distances for the high temperature phase of $Mn_{1.5}VO_4$, whose structure is illustrated in Fig. 4. Mn^{2+} is in a distorted octahedral coordination at the 8*c* and 8*d* sites, whereas V^{5+} is found in tetrahedral coordination with almost equal V–O distances, but with O–V–O angles deviating from the ideal tetrahedral angle of 109.45°. The deviations of these two coordination species from higher symmetry may well be understood according to Pauling's rules for edge sharing polyhedra. The Mn^{2+} ion on the 4*b* site is found in an unusual *[4+4]* coordination (Fig. 5); this coordination polyhedron is known as Hoard dodecahedron [40,46] and also as stella quadrangula and it is found in quite a few compounds [47,48]. The Mn–O distances are clearly too large compared to what would be expected according to the ionic radii [38] (Table 4). Nevertheless, such large *M*–O distances are also found for $Co_{1.5}AsO_4$, whose structure was determined using single crystal data [40]. In that case, a higher displacement parameter is found for the Co^{2+} ion on the central 4*b* position. An independent refinement of the thermal parameter in our case gave no indication of thermal or static disorder on that site although it is to be expected.

A DTA measurement (Fig. 6, all temperatures given as onset-temperatures) on the orthorhombic phase showed that the phase transition to tetragonal starts at a temperature around 946 °C. Melting of the sample starts at a temperature of 972 °C and the DTA measurement combined with XRD showed that both thermal processes are reversible. Anyway, since the phase transition is completely reconstructive (hexagonal→cubic close packing of the O^{2-} ions), the transition is rather sluggish at lower temperatures and the high temperature phase can be obtained by quick cooling.

Table 4
Comparison of the refined *M*–O distances of the high temperature phase of $Mn_{1.5}VO_4$ (space group $I\bar{4}2d$) to the sum of the ionic radii after Shannon [38] with *N* being the number of neighbors. The sum of ionic radii for fourfold coordinated Mn^{2+} was approximated by comparison with Mg^{2+} (∗).

Atom site/atom sort	*N*	Refined distance (Å)	Average *M*–O distance (Å)	Sum of ionic radii [38]
***8c*/*Mn*$^{2+}$**	2	2.188(3)	2.225	2.193
	2	2.211(4)		
	2	2.275(3)		
***8d*/*Mn*$^{2+}$**	2	2.109(3)	2.171	2.193
	2	2.163(3)		
	2	2.242(4)		
***4b*/*Mn*$^{2+}$**	4	2.296(4)	CN=4: 2.296 CN=8: 2.553	CN=4: 1.97∗ CN=8: 2.31
	4	2.810(3)		
***4a*/*V*$^{5+}$**	4	1.671(3)	1.671	1.715
***8d*/*V*$^{5+}$**	2	1.669(3)	1.696	1.725
	2	1.722(3)		

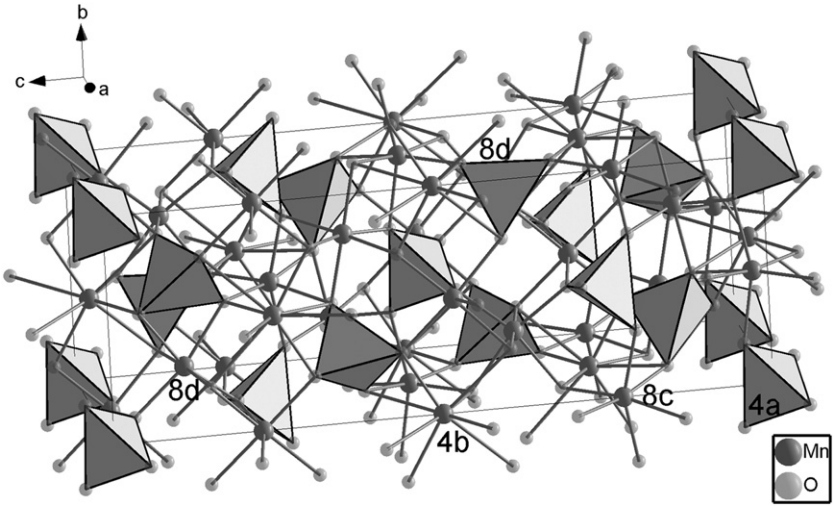

Fig. 4. The crystal structure of the tetragonal high temperature phase of $Mn_{1.5}VO_4$. Vanadium is located in the center of the filled tetrahedra.

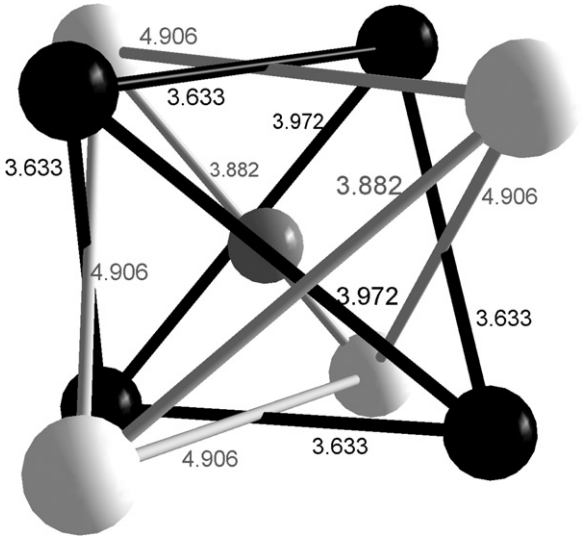

Fig. 5. The coordination sphere of the Mn^{2+} ion (dark gray) on the 4*b* site. The viewing direction is slightly shifted along the *c* axis. The Mn–O distance is 2.296 Å for the black and 2.810 Å for the gray oxygen atoms. O–O distances are given in Å.

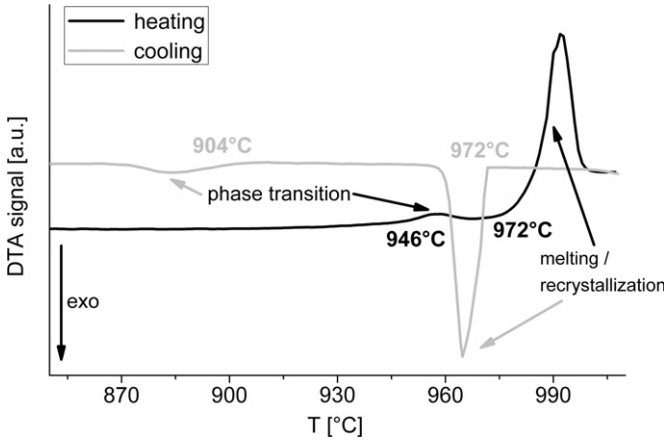

Fig. 6. DTA measurement on the orthorhombic modification of $Mn_{1.5}VO_4$. Temperatures are given as onset-temperatures.

In the presence of oxygen during heat treatment, the material decomposes under formation of $Mn_2V_2O_7$ and Mn_3O_4 in a first step. This emphasizes the importance of a high purity inert gas atmosphere. $Mn_2V_2O_7$ does not react further and Mn_3O_4, once formed, is not reduced back to MnO at our chosen reaction temperatures.

3.2. On $Li_xMn_{1.5-x/2}VO_4$ in the range $0 < x \leq 0.2$

On the manganese rich side of the system $LiMnVO_4$–$Mn_{1.5}VO_4$, i.e. $0 < x \leq 0.2$ in $Li_xMn_{1.5-x/2}VO_4$, the high temperature phase of

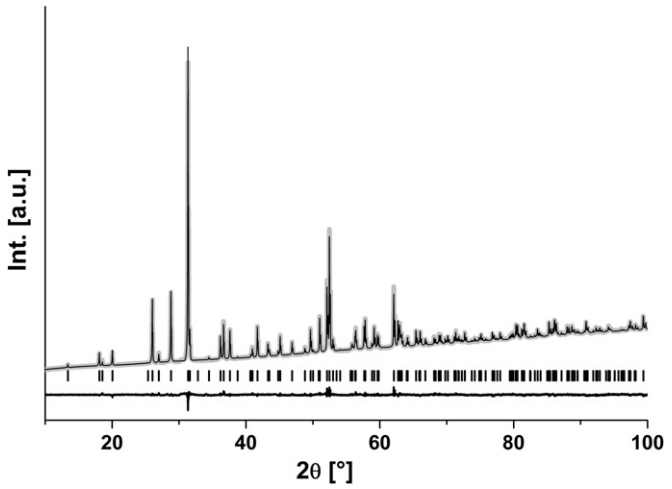

Fig. 7. Rietveld analysis of the XRD patterns of the synthesis product $Li_{0.2}Mn_{1.40}VO_4$. Refined curve (black), measured curve (gray) and difference curve (black). The background slope results from the varying divergence slit of the diffractometer.

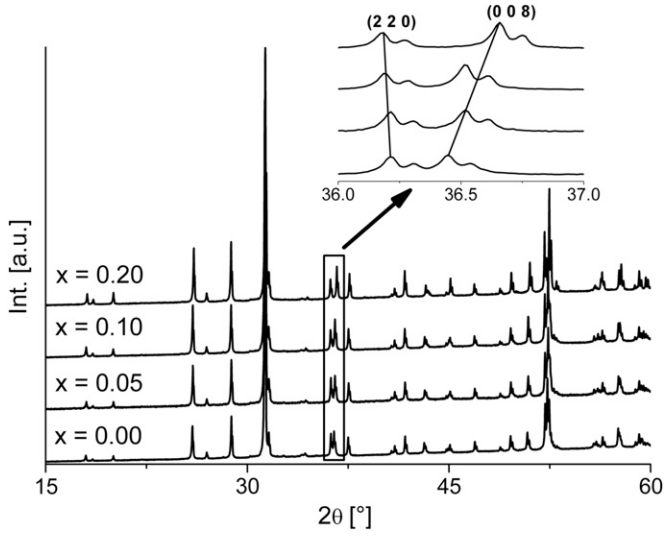

Fig. 8. XRD patterns of the system $Li_xMn_{1.5-x/2}VO_4$ for $0 \le x \le 0.2$. All compositions are found to crystallize in the tetragonal space group $I\bar{4}2d$. The inset shows the angle dependency of the (2 2 0) and the (0 0 8) reflections.

$Mn_{1.5}VO_4$ ($I\bar{4}2d$) is the only stable one (the refinement for $Li_{0.2}Mn_{1.40}VO_4$ is exemplarily shown in Fig. 7, an overview of the recorded XRD patterns is given in Fig. 8). Fig. 9 shows the variation of lattice parameters with composition. As one Mn^{2+} ion has to be substituted by two Li^+ ions, the half-filled 4*b* site in $Mn_{1.5}VO_4$ is an ideal candidate for this substitution process; the occupation of this site was therefore constrained to the formula $Li_xMn_{1.5-x/2}VO_4$ ($0 \le x \le 1/3$), whereas occupation of the other Mn sites was restricted to Mn^{2+} only. In contrast, such a substitution seems to be energetically unfavorable in the orthorhombic modification of $Mn_{1.5}VO_4$, since additional crystallographic sites would have to be occupied. We also found that the addition of small amounts of Li_3VO_4 forces orthorhombic $Mn_{1.5}VO_4$ to a structural transition into the tetragonal phase already at temperatures between 800 and 850 °C, which is about 80–130 °C below the observed phase transition temperature for $Mn_{1.5}VO_4$.

Although it is not possible to locate Li^+ ions by x-ray diffraction, occupation of the 4*b* site can be assumed from the similarity to the $AB_4(VO_4)_3$ structures mentioned above such as $Li_{1/3}Mg_{4/3}VO_4$ [43,44]

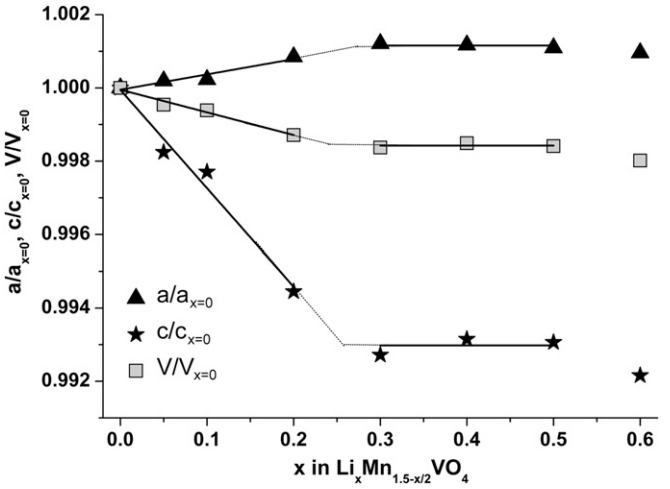

Fig. 9. Normalized lattice parameters and cell volume as function of the degree *x* of substitution in $Li_xMn_{1.5-x/2}VO_4$ (for $0.3 \le x \le 0.7$ two phase mixture of the tetragonal and an orthorhombic $LiMnVO_4$ like phase is obtained, see Sections 3.3 and 3.4).

Table 5
Results of the Rietveld refinements for the tetragonal ht-$Mn_{1.5}VO_4$ type phase (space group $I\bar{4}2d$) for the compositions $Li_xMn_{1.5-x/2}VO_4$ with $0 \le x \le 0.2$.

x in $Li_xMn_{1.5-x/2}VO_4$	*a* in Å	*c* in Å	Refined composition/refined *x*
0.00	7.0073(1)	19.6981(3)	$Mn_{1.497(4)}VO_4$
0.05	7.0088(1)	19.6641(4)	$x=0.05(2)$
0.10	7.0091(1)	19.6534(2)	$x=0.11(2)$
0.20	7.0135(1)	19.5893(3)	$x=0.25(2)$

and $Na_{1/3}Mg_{4/3}VO_4$[43], where the alkaline earth metal is also found in the Hoard dodecahedron. Furthermore, the inverse substitution is possible for $Li_{1/3}Mg_{4/3}VO_4$, following $Li_yMg_{1.5-y/2}VO_4$ in the range $0.2 \le y \le 0.3$ [45] and, in general, there seems to be a remarkable similarity between the systems Li_2O–MgO–V_2O_5 and Li_2O–MnO–V_2O_5 [39], as most compounds are isostructural to the corresponding compound of the accordant system. The refined compositions and site occupancies are in very good agreement with the suggested substitution mechanism.

When raising *x* to a value of 0.3, about 17 wt% orthorhombic $LiMnVO_4$ (space group *Cmcm*) are found as a second phase, which does not disappear after longer heat treatment. This indicates that a stoichiometric compound $Li_{1/3}Mn_{4/3}VO_4$ does not exist in this system. A more detailed determination of the miscibility gap is described in Section 3.4.

Substitution is accompanied by a decrease in unit cell volume for increasing x (Fig. 9). This might be explained by the smaller ionic radius of Li^+ compared to Mn^{2+} (0.74 vs. 0.82 Å for sixfold coordination [38]). The change of lattice parameters is not uniform. Whereas *c* decreases for increasing *x*, *a* slightly increases (see Figs. 9, 8 and Table 5). The Hoard dodecahedron is connected to four Mn^{2+} octahedra by edges within the a/b plane, whereas the edge connection to four V^{5+} tetrahedra is also directed with a component along [0 0 1] (Fig. 10). Therefore, the substitution of manganese by lithium lowers the repulsive forces between the 4*b* site and the V^{5+} site, which might contribute to the contraction of the structure in the *c* direction.

Again, equilibrating the sample with $x=0.1$ at 600 °C for 60 h causes a decomposition of the former single phased tetragonal material into orthorhombic $Mn_{1.5}VO_4$ (~17.2 wt%) and tetragonal $Li_xMn_{1.5-x/2}VO_4$ (~82.8 wt%). The latter can thereby be estimated to have an approximate composition $Li_{0.12}Mn_{1.44}VO_4$. In contrast, such a decomposition is not observed for $x=0.2$, which indicates

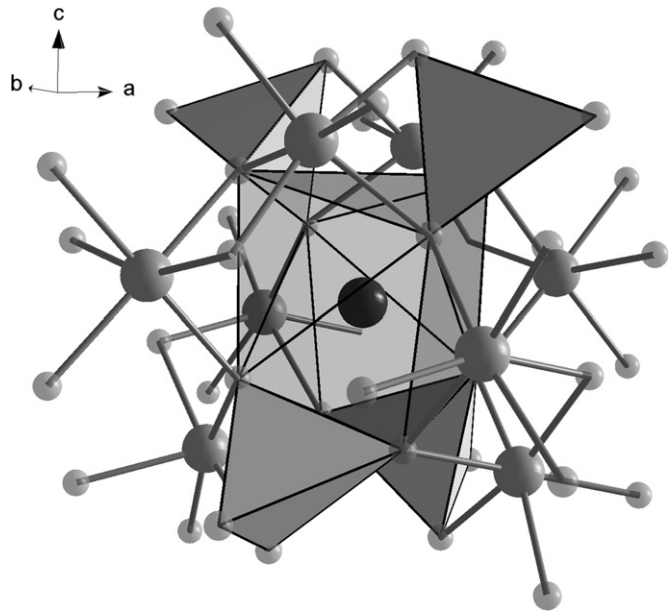

Fig. 10. Connection of the Hoard dodecahedron (4*b* position, black atom) to the neighboring polyhedra. Vanadium is located in the filled tetrahedra, other Mn^{2+} ions are plotted in dark gray color.

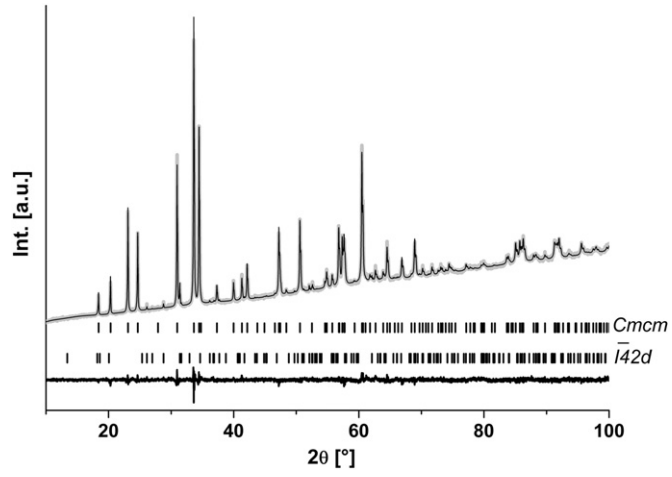

Fig. 11. Rietveld analysis of the XRD patterns of the synthesis product $Li_{0.7}Mn_{1.15}VO_4$. Refined curve (black), measured curve (gray) and difference curve (black). The background slope results from the varying divergence slit of the diffractometer.

that Li^+ acts in a way to stabilize the tetragonal phase at lower temperatures. This indicates that there is a reduced miscibility in the range $0 \le x \le \sim 0.1$, caused by a higher stability of the orthorhombic $Mn_{1.5}VO_4$ phase at lower temperatures. (It could also be possible – although not found experimentally – that the tetragonal phase is unstable at lower temperatures and transforms to orthorhombic $Mn_{1.5}VO_4$ (*Cmca*) and orthorhombic $Li_xMn_{1.5-x/2}VO_4$ (*Cmcm*, see Section 3.3). Since the formation of orthorhombic $Li_xMn_{1.5-x/2}VO_4$ (*Cmcm*) would also be accompanied by a complete structural reorganization, this could probably only be realized in very long firing times.)

3.3. On $Li_xMn_{1.5-x/2}VO_4$ in the range $0.7 < x \le 1.0$

Phases of this composition are found to crystallize in the orthorhombic space group *Cmcm*, adopting the structure of $LiMnVO_4$ [8] (the Rietveld refinement is exemplarily shown for $x=0.7$, see Fig. 11). The XRD patterns are shown in Fig. 12. For

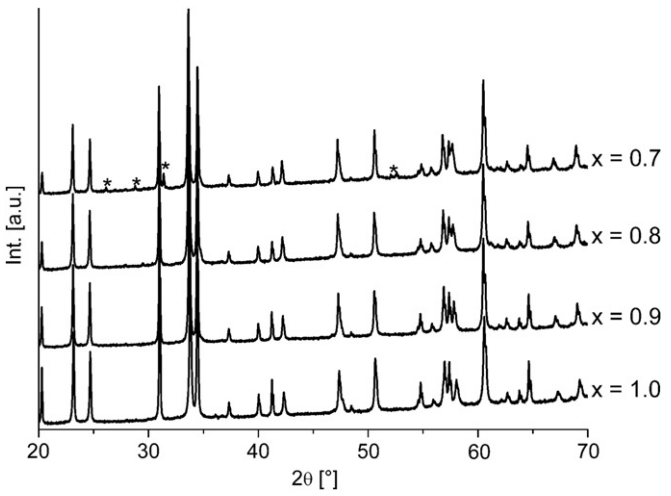

Fig. 12. XRD patterns of the system $Li_xMn_{1.5-x/2}VO_4$ for $0.7 \le x \le 1.0$. All compositions are found to crystallize in the orthorhombic space group *Cmcm*. The small amount of impurity phase (~3 wt%) of tetragonal $Li_xMn_{1.5-x/2}VO_4$ for $x=0.7$ is marked with asterisks.

Table 6
Results of the Rietveld refinements for the orthorhombic $LiMnVO_4$ type phase (space group *Cmcm*) for the compositions $Li_xMn_{1.5-x/2}VO_4$ with $0.7 \le x \le 1$.

x	*a* in (Å)	*b* in (Å)	*c* in (Å)	Refined *x*
1.0	5.7632(3)	8.7474(4)	6.3502(4)	*not constrained*
0.9	5.7644(2)	8.7507(3)	6.3724(2)	0.90(1)
0.8	5.7679(3)	8.7446(4)	6.3821(3)	0.84(2)
0.7	5.7715(2)	8.7337(3)	6.3899(2)	0.81(2)

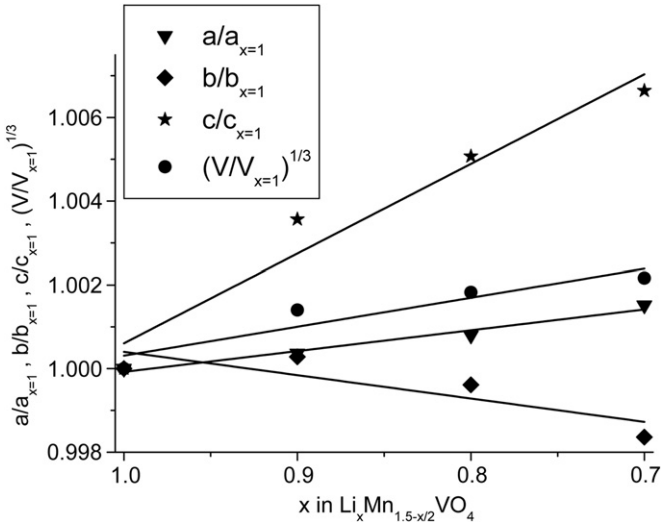

Fig. 13. Normalized lattice parameters and cell volume as function of the degree *x* of substitution in $Li_xMn_{1.5-x/2}VO_4$.

$x=0.7$, a small amount of tetragonal $Li_xMn_{1.5-x/2}VO_4$ is found (~3 wt%, see Fig. 11). Therefore, the miscibility gap is expected to lie close to the composition $Li_{0.7}Mn_{1.15}VO_4$).

Substitution leads to an increase of unit cell volume for decreasing *x* (Table 6, Fig. 13). This can be explained by the larger ionic radius of Mn^{2+} compared to Li^+ (0.82 vs. 0.74 Å for sixfold coordination [38], see above). Furthermore, the dependence of the lattice parameters on *x* is not uniform. For decreasing *x*, *a* and *c* both increase, whereas *b* slightly decreases. The Rietveld refinement indicates a substitution of two Li^+ ions on the 4*c* site by one

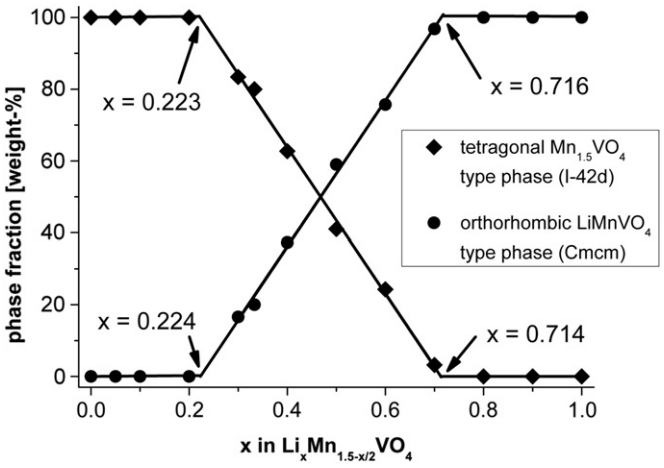

Fig. 14. Refined weight fractions of different phases in the synthesis of $Li_xMn_{1.5-x/2}VO_4$ compounds.

Mn^{2+} ion leaving one defect position. The Li^+/Mn^{2+} ions are in fourfold coordination on that site, sharing an edge with a vanadium tetrahedron along the *b* axis. Therefore, a shrinkage of the *b* axis, which causes a lowering of the Mn^{2+}–V^{5+} distance, is very small in the magnitude of about 0.1–0.2% (Fig. 14).

3.4. $Li_xMn_{1.5-x/2}VO_4$ ($0.3 \le x \le 0.7$)

The investigation of compositions with $0.3 \le x \le 0.7$ prepared at 900 °C shows the formation of a two phase mixture containing an orthorhombic $LiMnVO_4$ like (*Cmcm*) and a tetragonal $Mn_{1.5}VO_4$ like ($I\bar{4}2d$) compound. The refinement of relative amounts and lattice parameters of the phases existing in the range $0.3 \le x \le 0.6$ was performed by fixing the atomic positions and occupancies to the ones found earlier for $x=0.2$ and 0.7, respectively. For the tetragonal phase, the lattice parameters and the volume are nearly constant in this range and this indicates the beginning of the miscibility gap at $x \approx 0.24$ to 0.27 (see Fig. 9). The lattice parameters depicted in Fig. 9 were fitted by linear equations. The refined lattice parameters of the orthorhombic phase showed a complex behavior and could not be interpreted unambiguously. Nevertheless, the refined weight fractions give a clearer picture and indicate limits of doping around $Li_{0.22-0.23}Mn_{1.39-1.385}VO_4$ for the tetragonal phase and $Li_{0.71-0.72}Mn_{1.145-1.14}VO_4$ for the orthorhombic one, and this is in agreement with the beginning of the miscibility gap at the Mn richer side determined by the lattice parameters only. It needs to be taken into account that solid state preparations of the Li richer phases have to be done at lower temperatures due to a lower melting point.

The miscibility gap seems to be caused by an intolerance of $LiMnVO_4$ towards a high degree of Li substitution for Mn. This can be understood in view of the edge connectivity of the Li and V tetrahedra and the resulting higher repulsive forces of doubly charged Mn on this site. In principle the formation of a tetragonal compound $Li_{0.33}Mn_{1.33}VO_4$ should be possible without the occupation of further crystallographic sites by Li (see Section 3.2). The appearance of the orthorhombic $LiMnVO_4$ type phase for $x \ll 0.33$ might be explained either by its higher thermodynamic stability or by a lowering of Madelung energy in the tetragonal phase in the course of the substitution of the higher valent cation by the lower valent one.

4. Conclusions

In this paper, we have shown that orthorhombic $Mn_{1.5}VO_4$ (space group *Cmca*) can be prepared by a simple solid state route. A second former unknown modification of $Mn_{1.5}VO_4$ is found when heating the material to a temperature of 950 °C. This modification is isostructural to $Co_{1.5}AsO_4$ and $Mg_{1.5}AsO_4$ and crystallizes in the tetragonal space group $I\bar{4}2d$. The major part of Mn^{2+} (8/9) is found in octahedral coordination, whereas the rest is in an unusual *[4+4]* coordination called Hoard dodecahedron or stella quadrangula, with this special crystallographic site being half occupied. The phase transition back to orthorhombic is possible, but kinetically limited on quick cooling.

Substitution of Mn^{2+} for two Li^+ favors the formation of tetragonal $Li_xMn_{1.5-x/2}VO_4$ for $0 \le x \le 0.2$. The tetragonal structure facilitates such a substitution, as the Mn site with *[4+4]* coordination is only half occupied from the beginning on. Full exchange giving a final composition $Li_{1/3}Mn_{4/3}VO_4$, which would then be isostructural to $Li_{1/3}Mg_{4/3}VO_4$ [43–45] and $Na_{1/3}Mg_{4/3}VO_4$ [43], is not possible. Synthesis attempts of such a phase resulted in the formation of an additional $LiMnVO_4$ type phase (space group *Cmcm*). Furthermore, the substitution goes with shrinkage of cell volume, with decreasing *c*, but increasing *a* parameter. This can be explained by comparison of the ionic radii of Mn^{2+} and Li^+ and by the connectivity of the coordination polyhedra. Furthermore, a substitution following the scheme $Li_xMn_{1.5-x/2}VO_4$ is not found for orthorhombic $Mn_{1.5}VO_4$, not even for small values of *x*. This structure does not allow such a substitution, since additional crystallographic sites would have to be occupied.

For $0.7 \le x \le 1.0$, the samples are found to crystallize in the orthorhombic structure of $LiMnVO_4$ (space group *Cmcm*). One Mn^{2+} is found to substitute two Li^+ on the tetrahedrally coordinated 4*c* site, leaving also vacancies on this site.

When trying to synthesize samples in the range $0.3 \le x \le 0.7$, we found two phase mixtures of tetragonal and orthorhombic phases mentioned afore. Rietveld refinement of the phase ratios showed that at temperatures between 850 and 940 °C there is a miscibility gap between $Li_{0.22-0.23}Mn_{1.39-1.385}VO_4$ on the tetragonal and $Li_{0.71-0.72}Mn_{1.145-1.14}VO_4$ on the orthorhombic side.

Acknowledgments

Oliver Clemens wants to thank the "Landesgraduiertenförderung Saarland" for financial support and Isabell Omlor for help in synthetic work.

Appendix A. Supplementary materials

Supplementary materials associated with this article can be found in the online version at doi:10.1016/j.jssc.2011.07.042.

References

[1] A. Yamada, H. Koizumi, S. Nishimura, N. Sonoyama, R. Kanno, M. Yonemura, T. Nakamura, Y. Kobayashi, Nat. Mater. 5 (2006) 357–360.
[2] A.K. Padhi, K.S. Nanjundaswamy, J.B. Goodenough, J. Electrochem. Soc. 144 (1997) 1188–1194.
[3] D. Morgan, A.V.d. Ven, G. Ceder, Electrochem. Solid-State Lett. 7 (2004) A30–A32.
[4] J.M. Osorio-Guillén, B. Holm, R. Ahuja, B. Johansson, Solid State Ionics 164 (2004) 221–227.
[5] H. Ehrenberg, N.N. Bramnik, A. Senyshyn, H. Fuess, Solid State Sci. 11 (2009) 18–23.
[6] C.H. Mi, X.G. Zhang, X.B. Zhao, H.L. Li, Mater. Sci. Eng. B 129 (2006) 8–13.
[7] A. Yamada, M. Hosoya, S.-C. Chung, Y. Kudo, K. Hinokuma, K.-Y. Liu, Y. Nishi, J. Power Sources 119–121 (2003) 232–238.
[8] A.K. Padhi, W.B. Archibald, K.S. Nanjundaswamy, J.B. Goodenough, J. Solid State Chem. 128 (1997) 267–272.
[9] S. Suzuki, M. Tomita, S. Okadas, H. Arai, J. Phys. Chem. Solids 58 (1997) 799–805.
[10] M.-T. Paques-Ledent, Chem. Phys. Lett. 35 (1975) 375–378.

[11] K. Rissouli, K. Benkhouja, M. Touaiher, A.A. Salah, K. Jaafari, M. Fahad, C. Julien, J. Phys. IV 123 (2005) 265–269.
[12] M. Sato, S. Kano, S. Tamaki, M. Misawa, Y. Shirakawa, M. Ohashi, J. Mater. Chem. 6 (1996) 1191–1194.
[13] M. Sugahara, A. Yoshiasa, T. Yamanaka, H. Takei, Acta Crystallogr. E59 (2003) i161–i163.
[14] M.T. Paques-Ledent, P. Tarte, Spectrochim. Acta Part A 30 (1974) 673–689.
[15] M. Xing, W. Chun-Zhong, F. Hou-Gang, H. Fang, W. Ying-Jin, H. Zu-Fei, M. Xing, C. Gang, J. Phys.: Condens. Matter (2008) 395204.
[16] L.L.Y. Chang, F.Y. Wang, J. Am. Ceram. Soc. 71 (1988) 689–693.
[17] G. Blasse, J. Inorg. Nucl. Chem. 25 (1963) 230–231.
[18] D. Capsoni, M. Bini, V. Massarotti, P. Mustarelli, F. Belotti, P. Galinetto, J. Phys. Chem. B 110 (2006) 5409–5415.
[19] M. Touboul, A. Popot, J. Solid State Chem. 65 (1986) 287–292.
[20] G.T.-K. Fey, D.-L. Huang, Electrochim. Acta 45 (1999) 295–314.
[21] J. Shirakawa, M. Nakayama, H. Ikuta, Y. Uchimoto, M. Wakihara, Electrochem. Solid-State Lett. 7 (2004) A27–A29.
[22] Q.Y. Lai, J.Z. Lu, X.B. Su, X.Y. Ji, J. Solid State Chem. 165 (2002) 312–316.
[23] R.S. Liu, Y.C. Cheng, R. Gundakaram, L.Y. Jang, Mater. Res. Bull. 36 (2001) 1479–1486.
[24] C. Delacourt, L. Laffont, R. Bouchet, C. Wurm, J.B. Leriche, M. Morcrette, J.M. Tarascon, C. Masquelier, J. Electrochem. Soc. 152 (2005) A913–A921.
[25] G.M. Clark, R. Morley, A.N. Pick, J. Inorg. Nucl. Chem. 39 (1977) 1841–1843.
[26] C. Brisi, Ann. Chim. Rome 48 (1958) 270.
[27] X. Wang, Z. Liu, A. Ambrosini, A. Maignan, C.L. Stern, K.R. Poeppelmeier, V.P. Dravid, Solid State Sci. 2 (2000) 99–107.
[28] A.G. Nord, G. Aberg, Chem. Scr. 25 (1985) 212–216.
[29] A.G. Nord, P.-E. Werner, Z. Kristallogr. 149 (1991) 49–55.
[30] P.L. Wang, P.-E. Werner, A.G. Nord, Z. Kristallogr. 198 (1992) 271–276.
[31] E.E. Sauerbrei, R. Faggiani, C. Calvo, Acta Crystallogr. B29 (1973) 2304–2306.
[32] H. Fuess, E.F. Bertaut, R. Pauthenet, A. Durif, Acta Crystallogr. B26 (1970) 2036–2046.
[33] N. Qureshi, H. Fuess, H. Ehrenberg, T.C. Hansen, C. Ritter, K. Prokes, A. Podlesnyak, D. Schwabe, Phys. Rev. B: Condens. Matter Mater. Phys. 74 (2006) 212407.
[34] Topas V2.1, General profile and structure analysis software for powder diffraction data, User Manual. Bruker AXS, Karlsruhe, 2003.
[35] R.W. Cheary, A.A. Coelho, J.P. Cline, J. Res. Nat. Inst. Stand. Technol. 109 (2004) 1–25.
[36] A.A. Coelho, J. Appl. Crystallogr. 36 (2003) 86–95.
[37] Topas V4.2, General profile and structure analysis software for powder diffraction data, User's Manual. Bruker AXS, Karlsruhe, 2008.
[38] R.D. Shannon, Acta Crystallogr. A32 (1976) 751–767.
[39] P. Villars, K. Cenzual, *Pearson's Crystal Data: Crystal Structure Database for Inorganic Compounds*. Version 1.0 ed.; ASM International®, Materials Park, Ohio, 2007.
[40] R. Gopal, J.S. Rutherford, B.E. Robertson, J. Solid State Chem. 32 (1980) 29–40.
[41] N. Krishnamachari, C. Calvo, Acta Crystallogr. B29 (1973) 2611–2613.
[42] H.A. Anissa, A. Brahim, H. Hamor, Acta Crystallogr. E60 (2004) i77–i79.
[43] B.V. Slobodin, L.L. Surat, Inorg. Mater. 40 (2004) 188–194.
[44] A.P. Tyutyunnik, V.G. Zubkov, L.L. Surat, B.V. Slobodin, Russ. J. Inorg. Chem. 49 (2004) 610–616.
[45] G. Torres-Trevino, E.E. Lachowski, A.R. West, J. Mater. Sci. Lett. 5 (1986) 615–616.
[46] J.L. Hoard, J.V. Silverton, Inorg. Chem. 2 (1963) 235–242.
[47] H. Nyman, S. Andersson, Acta Crystallogr. A35 (1979) 934–937.
[48] U. Wedig, V. Saltykov, J.r. Nuss, M. Jansen, J. Am. Chem. Soc. 132 (2010) 12458–12463.